Reversible Thermal-Mode Control of Luminescence from Liquid-Crystalline Gold(I) Complexes

Kaori Fujisawa,[a,b] Yuki Okuda,[a] Yuichi Izumi,[a] Akira Nagamatsu,[a] Yuki Rokusha,[a] Yusuke Sadaike,[a] Osamu Tsutsumi[a,*]

[a]Department of Applied Chemistry, College of Life Sciences, Ritsumeikan University, 1-1-1 Nojihigashi, Kusatsu 525-8577, Japan. Fax: +81-77-561-2659; Tel: +81-77-561-5966.

[b]Present address: Department of Organic Chemistry, University of Geneva.

*tsutsumi@sk.ritsumei.ac.jp

Table of Contents

1. Synthesis of Isocyanide Ligands

General Methods. Ligand **S4** was synthesized according to reported procedures (Scheme 1). Unless otherwise noted, all solvents and reagents were purchased from commercial suppliers and were used without further purification. ^{1}H NMR spectra were recorded on a JEOL ECS-400 spectrometer at 400 MHz using the residual proton in the NMR solvent as an internal reference. Electrospray ionization mass spectra (ESI-MS) were recorded on a JMS-T1000LC (JEOL) mass spectrometer. MALDI-TOF mass spectra were recorded on a Bruker Autoflex II instrument with dithranol (Aldrich) as the matrix. Infrared (IR) spectra were recorded on a JASCO FT/IR-4100 spectrometer using KBr pellets.

Scheme 1. Synthetic route for isocyanide ligands[1,2]

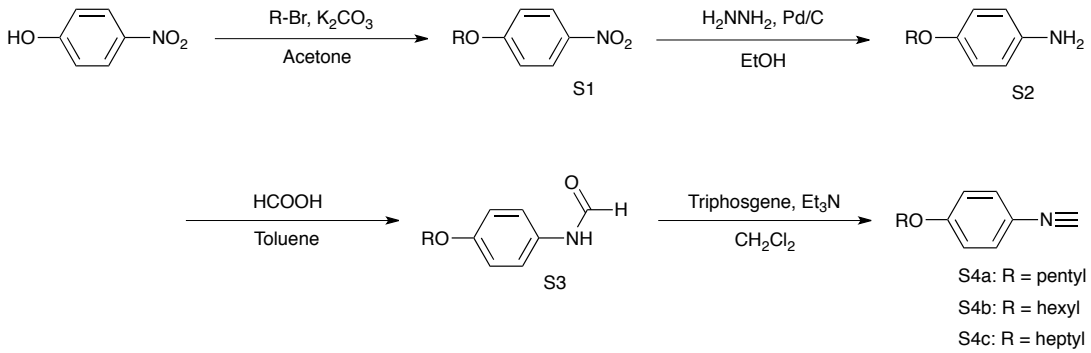

Synthesis of 1-nitro-4-alkoxybenzenes (S1).

S1a: 4-Nitrophenol (5.1 g, 36 mmol), potassium carbonate (9.9 g, 72 mmol), 18-crown-6 (189 mg, 0.72 mmol), and 1-bromopentane (8.9 mL, 72 mmol) were added to acetone (70 mL) and the reaction mixture was refluxed overnight. The solid was filtered off and the filtrate was concentrated by evaporation. The residue was dissolved in diethyl ether and washed with water and brine. The organic layer was dried over anhydrous sodium sulphate and concentrated by evaporation. The crude product was purified on a silica gel column (*n*-hexane/ethyl acetate = 98/2) to obtain **S1a** (4.3 g, 21 mmol) in 57% yield. ^{1}H NMR (400 MHz, $CDCl_3$): δ 8.17 (dd, J = 7.1 and 2.1 Hz, 2H, 3,5-H in benzene), 6.92 (dd, J = 7.1 and 2.1 Hz, 2H, 2,6-H in benzene), 4.03 (t, J = 6.6 Hz, 2H, OCH_2), 1.81 (quin, J = 6.7 Hz, 2H, OCH_2CH_2), 1.48–1.33 (m, 4H, CH_2), 0.93 (t, J = 7.1 Hz, 3H, CH_3).

S1b and S1c. Based on the above procedure, **S1b** and **S1c** were obtained in 52% and 77% yields, respectively.

S1b: ^{1}H NMR (400 MHz, $CDCl_3$): δ 8.19 (dd, J = 7.1 and 2.1 Hz, 2H, 3,5-H in

benzene), 6.94 (dd, J = 7.1 and 2.1 Hz, 2H, 2,6-H in benzene), 4.04 (t, J = 6.6 Hz, 2H, OCH_2), 1.81 (quin, J = 6.7 Hz, 2H, OCH_2CH_2), 1.49–1.32 (m, 6H, CH_2), 0.91 (t, J = 7.0 Hz, 3H, CH_3).

S1c: ^{1}H NMR (400 MHz, $CDCl_3$): δ 8.18 (dd, J = 7.1 and 2.1 Hz, 2H, 3,5-H in benzene), 6.92 (dd, J = 7.1 and 2.1 Hz, 2H, 2,6-H in benzene), 4.03 (t, J = 6.6 Hz, 2H, OCH_2), 1.80 (quin, J = 6.7 Hz, 2H, OCH_2CH_2), 1.53–1.21 (m, 8H, CH_2), 0.88 (t, J = 7 Hz, 3H, CH_3).

Synthesis of 4-alkoxyanilines (S2).

S2a: Hydrazine monohydrate (17 mL, 360 mmol) and 5% palladium on carbon (2.9 g, 25 mmol) were added to a solution of 1-nitro-4-pentyloxybenzene (**S1a**; 2.4 g, 12 mmol) in EtOH (730 mL). The reaction mixture was refluxed overnight under argon. The solid was filtered off, and the filtrate was concentrated by evaporation. The residue was dissolved in diethyl ether and washed with water and brine. The organic layer was dried over anhydrous sodium sulphate, and the solvent was removed under reduced pressure to obtain **S2a** (1.6 g, 8.9 mmol) in 74% yield. ^{1}H NMR (400 MHz, $CDCl_3$): δ 6.75 (dd, J = 6.8 and 2.3 Hz, 2H, 3,5-H in benzene), 6.64 (dd, J = 6.8 and 2.3 Hz, 2H, 2,6-H in benzene), 3.88 (t, J = 6.6 Hz, 2H, OCH_2), 3.33 (s, 2H, NH_2), 1.75 (quin, J = 6.6 Hz, 2H, OCH_2CH_2), 1.54–1.33 (m, 4H, CH_2), 0.92 (t, J = 7.1 Hz, 3H, CH_3).

S2b and S2c. Based on the above procedure, **S2b** and **S2c** were obtained in 69% and 85% yields, respectively.

S2b: ^{1}H NMR (400 MHz, $CDCl_3$): δ 6.74 (dd, J = 6.6 and 2.3 Hz, 2H, 3,5-H in benzene), 6.64 (dd, J = 6.6 and 2.3 Hz, 2H, 2,6-H in benzene), 3.88 (t, J = 6.6 Hz, 2H, OCH_2), 3.41 (s, 2H, NH_2), 1.74 (quin, J = 6.8 Hz, 2H, OCH_2CH_2), 1.51–1.23 (m, 6H, CH_2), 0.90 (t, J = 6.9 Hz, 3H, CH_3).

S2c: ^{1}H NMR (400 MHz, CD_2Cl_2): δ 6.68 (dd, J = 6.6 and 2.1 Hz, 2H, 3,5-H in benzene), 6.58 (dd, J = 6.6 and 2.1 Hz, 2H, 2,6-H in benzene), 3.83 (t, J = 6.6 Hz, 2H, OCH_2), 3.41 (s, 2H, NH_2), 1.70 (quin, J = 6.6 Hz, 2H, OCH_2CH_2), 1.48–1.22 (m, 8H, CH_2), 0.87 (d, J = 6.6 Hz, 3H, CH_3).

Synthesis of *N*-(4-alkoxyphenyl)formamides (S3).

S3a: 4-Pentyloxyaniline (**S2a**; 1.0 g, 5.6 mmol) and formic acid (3.3 g, 73 mmol) were dissolved in toluene (34 mL) and the reaction mixture was refluxed under argon for 4 h, diluted with dichloromethane and washed with water and brine. The organic layer was dried over anhydrous sodium sulphate and concentrated under reduced pressure to obtain **S3a** (0.29 g,

1.4 mmol) in 24% yield. ^{1}H NMR (400 MHz, $CDCl_3$): δ 8.49 (d, J = 11.6 Hz, 0.5H, CHO, *cis*), 8.32 (d, J = 1.8 Hz, 0.5H, CHO, *trans*), 7.73 (s, 0.5H, NH, *cis*), 7.43 (dd, J = 6.9 and 2.4 Hz, 1H, 2,5-H in benzene, *trans*), 7.19 (s, 0.5H, NH, *trans*), 7.01 (dd, J = 7.1 and 2.2 Hz, 1H, 2,5-H in benzene, *cis*), 6.94–6.80 (m, 2H, 3,6-H in benzene), 3.93 (t, J = 6.6 Hz, 2H, OCH_2), 1.86–1.64 (m, 2H, OCH_2CH_2), 1.51–1.31 (m, 4H, CH_2), 0.93 (t, J = 7.1 Hz, 3H, CH_3).

S3b and S3c. Based on the above procedure, **S3b** and **S3c** were obtained in 97% and 67% yields, respectively.

S3b: ^{1}H NMR (400 MHz, $CDCl_3$): δ 8.48 (d, J = 11.5 Hz, 0.5H, CHO, *cis*), 8.31 (d, J = 1.9 Hz, 0.5H, CHO, *trans*), 7.89 (s, 0.5H, NH, *cis*), 7.41 (dd, J = 6.7 and 2.3 Hz, 1H, 2,5-H in benzene, *trans*), 7.25 (s, 0.5H, NH, *trans*), 7.00 (dd, J = 7.0 and 2.3 Hz, 1H, 2,5-H in benzene, *cis*), 6.93–6.78 (m, 2H, 3,6-H in benzene), 3.92 (t, J = 6.6 Hz, 2H, OCH_2), 1.80–1.72 (m, 2H, OCH_2CH_2), 1.52–1.25 (m, 6H, CH_2), 0.89 (t, J = 7.4 Hz, 3H, CH_3).

S3c: ^{1}H NMR (400 MHz, CD_2Cl_2): δ 8.47 (d, J = 11.6 Hz, 0.5H, CHO, *cis*), 8.26 (d, J = 1.8 Hz, 0.5H, CHO, *trans*), 7.53 (s, 0.5H, NH, *cis*), 7.40 (dd, J = 7.5 and 2.3 Hz, 1H, 2,5-H in benzene, *trans*), 7.18 (s, 0.5H, NH, *trans*), 7.00 (dd, J = 6.8 and 1.9 Hz, 1H, 2,5-H in benzene, *cis*), 6.89–6.80 (m, 2H, 3,6-H in benzene), 3.91 (t, J = 6.6 Hz, 2H, OCH_2), 1.82–1.65 (m, 2H, OCH_2CH_2), 1.47–1.10 (m, 8H, CH_2), 0.88 (t, J = 6.7 Hz, 3H, CH_3).

Synthesis of 4-alkoxyphenyl isocyanides (S4).

S4a: Triphosgene (137 mg 0.46 mmol), *N*-(4-pentyloxyphenyl)formamide (290 mg 1.40 mmol) and triethylamine (5.9 mL, 4.2 mmol) were dissolved in dichloromethane (6.7 mL). The solution was stirred for 1 h at room temperature, the solvents were evaporated and the residue was purified on a silica gel column (hexane/dichloromethane = 3/1) to obtain **S4a** (92 mg, 0.48 mmol, 35% yield). ^{1}H NMR (400 MHz, $CDCl_3$): δ 7.24 (dd, J = 7.0 and 1.9 Hz, 2H, 3,5-H in benzene), 6.82 (dd, J = 7.0 and 1.9 Hz, 2H, 2,6-H in benzene), 3.91 (t, J = 7.0 Hz, 2H, OCH_2), 1.75 (quin, J = 7.0 Hz, 2H, OCH_2CH_2), 1.45–1.30 (m, 4H, CH_2), 0.90 (t, J = 7.0 Hz, 3H, CH_3).

S4b and S4c. Based on the above procedure, **S4b** and **S4c** were obtained in 84% and 23% yields, respectively.

S4b: ^{1}H NMR (400 MHz, $CDCl_3$): δ 7.27 (dd, J = 7.1 and 1.9 Hz, 2H, 2,6-H in benzene) 6.83 (d, J = 7.1 and 1.9 Hz, 2H, 3,5-H in benzene), 3.93 (t, J = 7.0 Hz, 2H, OCH_2), 1.75 (quin, J = 7.0 Hz, 2H, OCH_2CH_2) 1.47–1.24 (m, 6H, CH_2), 0.89 (t, J = 6.6 Hz, 3H, CH_3).

S4c: ^{1}H NMR (400 MHz, $CDCl_3$): δ 7.28 (dd, J = 6.8 and 2.0 Hz, 2H, 3,5-H in

benzene), 6.82 (dd, J = 6.8 and 2.0 Hz, 2H, 2,6-H in benzene), 3.92 (t, J = 6.6 Hz, 2H, OCH_2), 1.74 (quin, J = 6.6 Hz, 2H, OCH_2CH_2), 1.48–1.20 (m, 8H, CH_2), 0.86 (t, J = 6.8 Hz, 3H, CH_3).

2. Thermodynamic properties.

Thermal stability of the complexes was evaluated by thermogravimetric analysis (TGA; Shimadzu, DTG-60AH) at a heating rate of 5 °C/min (Fig. S1). The decomposition temperatures were 253 °C for **1a**, 254 °C for **1b**, and 262 °C for **1c**.

Liquid-crystalline (LC) behaviour of the complexes was observed on an Olympus, BX51 polarizing microscope equipped with an Instec HCS302 hot-stage and an mK1000 controller. The thermodynamic properties of LCs were determined by differential scanning calorimetry (DSC; SII X-DSC7000) at a heating and cooling rate of 2.0 ℃/min (Fig. S2). At least three scans were performed to ensure reproducibility.

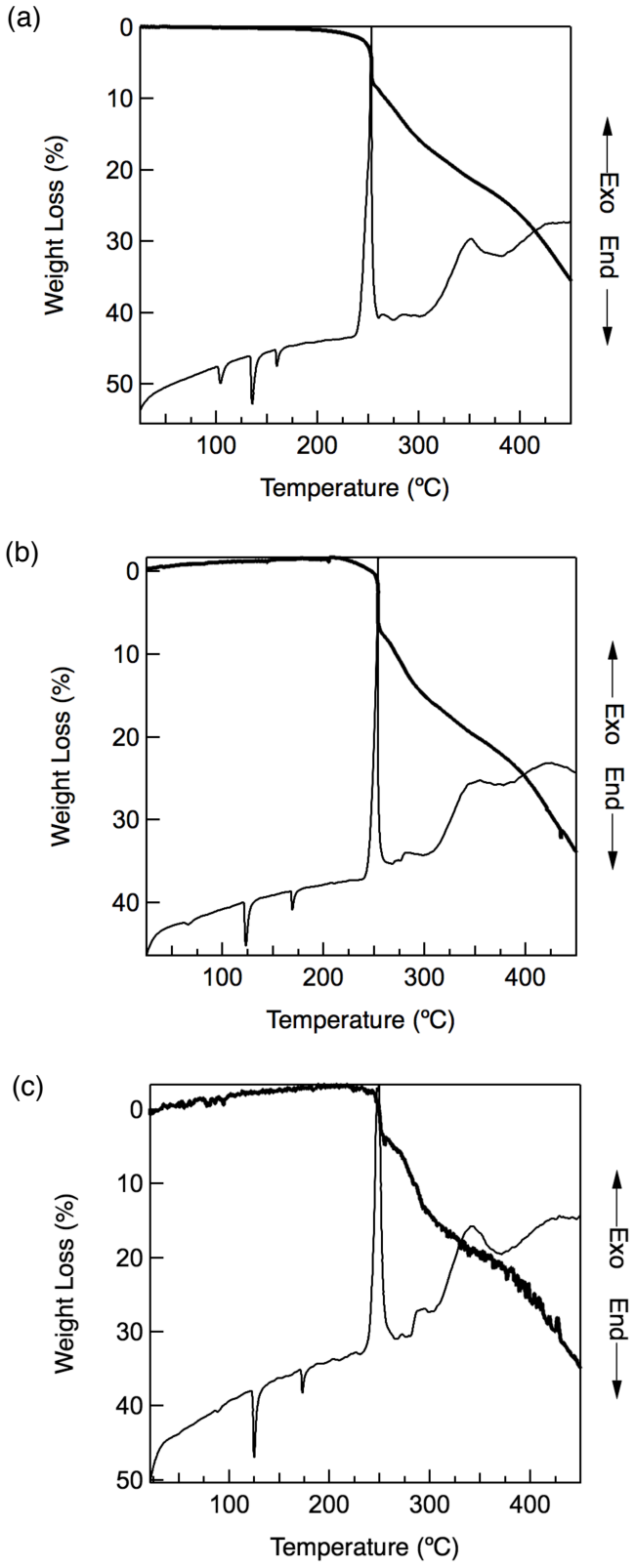

Fig. S1. Thermogravimetric analysis (thick line, left axis) and differential thermal analysis (thin line, right axis) thermograms of **1a** (a), **1b** (b), and **1c** (c). Scan rate was 5 ºC/ min.

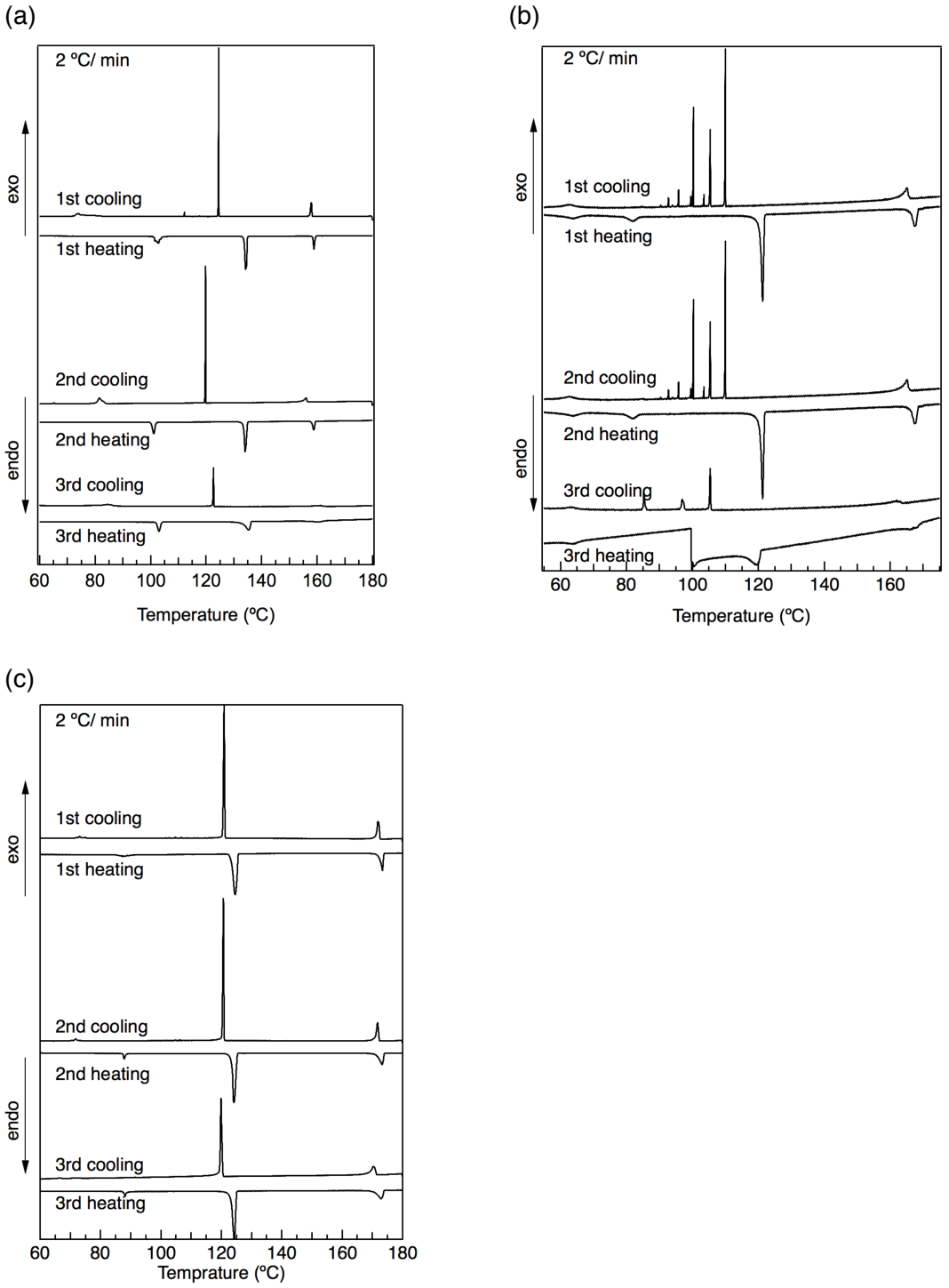

Fig. S2. Differential scanning calorimetry thermograms of **1a** (a), **1b** (b), and **1c** (c).

3. X-ray Crystallography.

Single crystals were obtained by slow evaporation from benzene/heptane = 1/1 solution. The X-ray diffraction measurement was carried out at room temperature (296 K). The crystallographic data obtained are summarized in Table S2. Notably, when the alkyl chains were disordered, the atom occupancies were separated into two parts. The data have been indexed and included in the Cambridge Crystallographic Centre (CCDC) database under the following reference numbers: CCDC 965149 for **1a**, CCDC 965149 for **1b**, and CCDC 965150 for **1c**. The indexed database contains additional supplementary crystallographic data for this paper and may be accessed without charge at http://www.ccdc.cam.ac.uk/conts/retrieving.html. The CCDC may contacted by mail at 12, Union Road, Cambridge CB2 1EZ, U.K., by fax at (44)1223-336-033, or by e-mail at deposit@ccdc.cam.ac.uk.

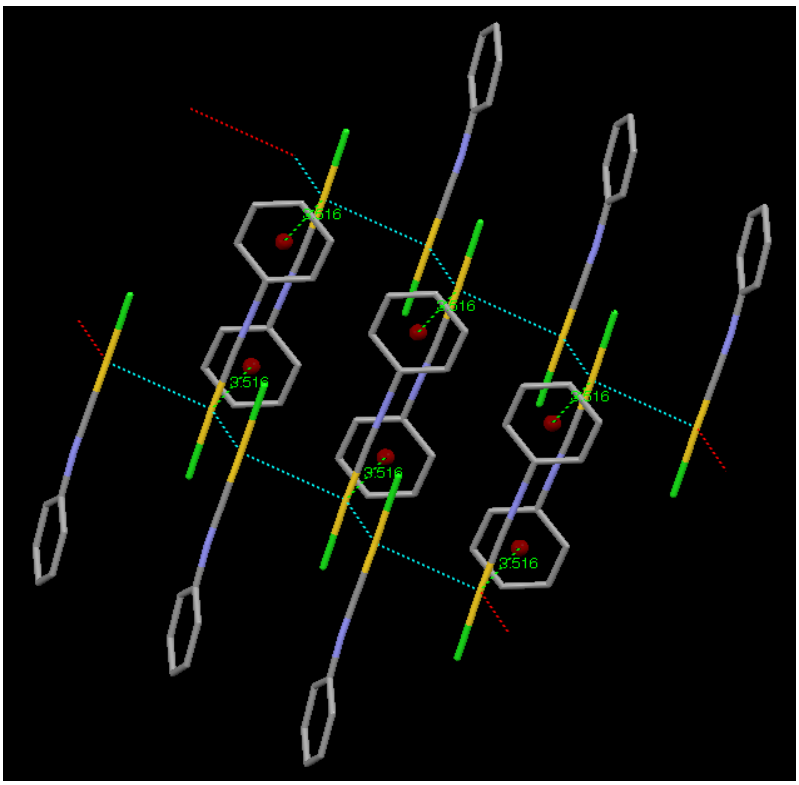

Fig. S3. Stick representation of crystal packing structure of complex **1b** at room temperature. For clarity, protons and alkoxy chains are omitted. Grey, C; green, Cl; purple, N; yellow, Au.

Table S1. Crystal data of complexes **1a–c**.

	1a	**1b**	**1c**
Radiation	Cu Kα	Cu Kα	Mo Kα
Empirical Formula	$C_{12}H_{15}AuClNO$	$C_{13}H_{17}AuClNO$	$C_{14}H_{19}AuClNO$
Formula Weight	421.67	435.69	449.73
Temperature	296 K	296 K	296 K
Crystal Colour, Habit	colourless, plate	colourless, block	colourless, prism
Crystal Dimensions (mm)	0.45 × 0.14 × 0.03	0.69 × 0.08 × 0.06	0.25 × 0.13 × 0.13
Crystal System	Monoclinic	Monoclinic	Triclinic
$R[F^2 > 2\sigma(F^2)]$	0.031	0.043	0.031
$wR(F^2)$	0.093	0.125	0.058
S	1.18	1.08	1.18
Space Group	$P2_1/a$	$P2_1/a$	P-1
Z	4	8	4
a (Å)	15.307 (3)	20.744 (2)	7.3185 (15)
b (Å)	5.912 (2)	7.279 (3)	10.594 (2)
c (Å)	15.3931 (17)	21.511(3)	20.763 (5)
α (º)	–	–	83.909 (8)
β (º)	106.796 (12)	116.686 (8)	81.684 (8)
γ (º)	–	–	75.894 (6)
V (Å^3)	1333.6 (5)	2902.1 (13)	1540.6 (6)

4. XRD in crystalline and liquid crystalline phase.

To determine the LC phase structure, powder X-ray diffractometry (XRD) was performed on Rigaku Ultima IV, XRD-DSC II. The XRD patterns of **1b** are shown in the main text (Fig. 4).

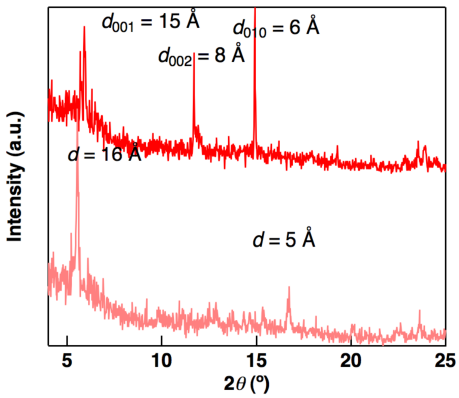

Fig. S4. X-ray diffraction patterns of **1a** in Cr_1 phase at 25 °C (red), and Cr_2 phase at 110 °C (pink) observed in the first heating process.

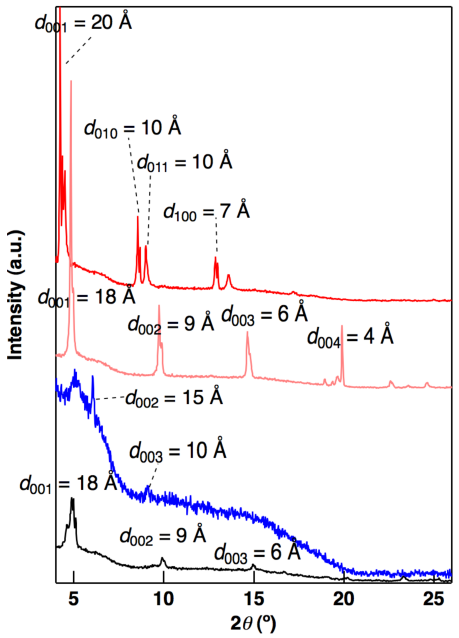

Fig. S5. X-ray diffraction patterns of **1c** in Cr_1 phase at 27 °C (red), Cr_2 phase at 100 °C (pink), SmC phase at 132 °C (blue), and Cr_2 phase at 25 °C in cooling process (supercooling) (black).

Table S2. Interlayer spacing and tilt angle of Sm phase.

	Interlayer spacing (Å)	Length of mesogen (Å)	Tilt angle (°)
1a	not determined[a]	27.3	–[a]
1b	27	32.2	33
1c	30	34.5	30

[a] XRD could not be measured.

5. Photophysical properties.

UV-Vis absorption and steady-state photoluminescence spectra were recorded on a JASCO V-550 absorption spectrophotometer and a Hitachi F-7500 fluorescence spectrophotometer, respectively. Photoluminescent quantum yields were determined by a calibrated integrating sphere system (Hitachi). Photoluminescent decay profiles were measured by using a nitrogen laser (USHO PULSED DYE LASER, KEC-160, λ = 337 nm, pulse width 600 ps, 10 Hz). The emission profiles were recorded with a streak camera (Hamamatsu, C4334).

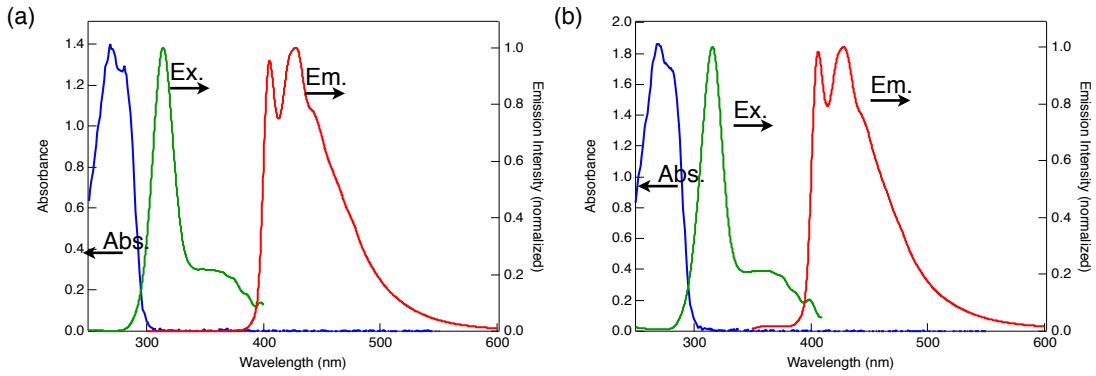

Fig. S6. Absorption, photoluminescence and excitation spectra of complex **1a** (a) and **1c** (b): absorption spectrum in CH_2Cl_2 solution (1×10^{-4} mol L^{-1}) (blue); photoluminescence in crystalline phase (λ_{ex} = 310 nm) (red); excitation spectrum in crystal (λ_{em} = 430 nm) (green).

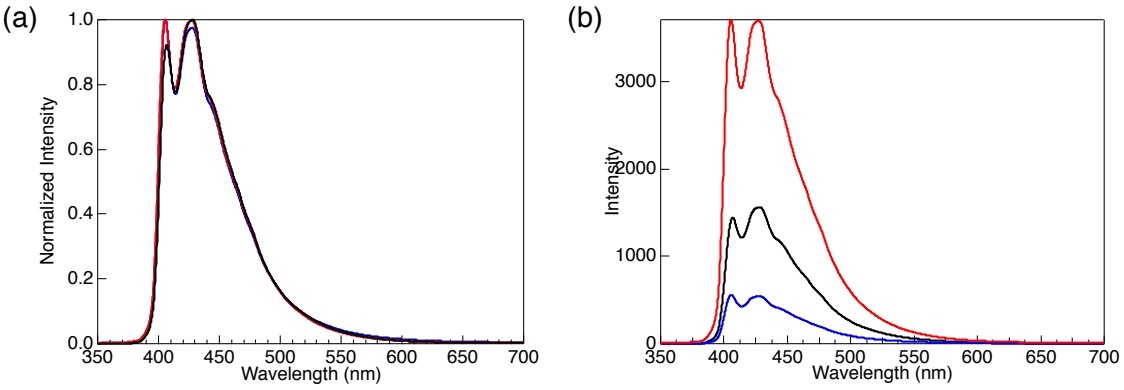

Fig. S7. Normalized (a) and original (b) photoluminescence spectra (excitation at 310 nm) of **1a** in Cr_1 at 30 °C (red), Sm at 140 °C (blue), and Cr at 30 °C (black).

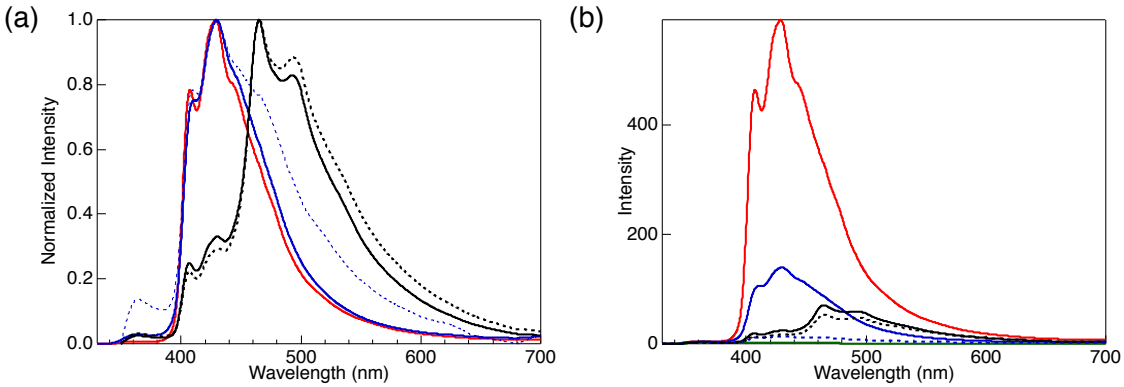

Fig. S8. Normalized (a) and original (b) photoluminescence spectra (excitation at 310 nm) of **1b** in Cr_1 at 40 °C (red), SmC at 130 °C (blue), I at 180 °C (green), and Cr_x at 40 °C (black). Broken lines indicate the second heating and cooling cycle.

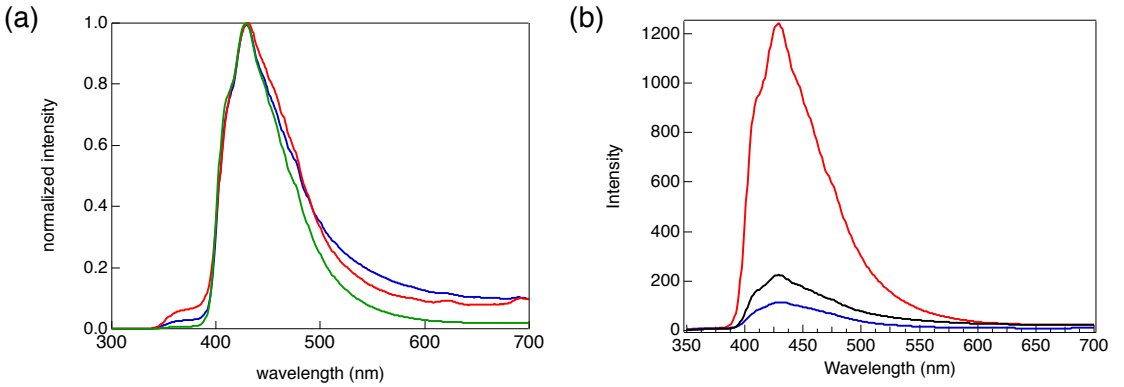

Fig. S9. Normalized (a) and original (b) photoluminescence spectra (excitation at 310 nm) of **1c** in Cr_1 at 30 °C (red), SmC at 130 °C (blue), and Cr_2 at 30 °C (supercooling) (black).

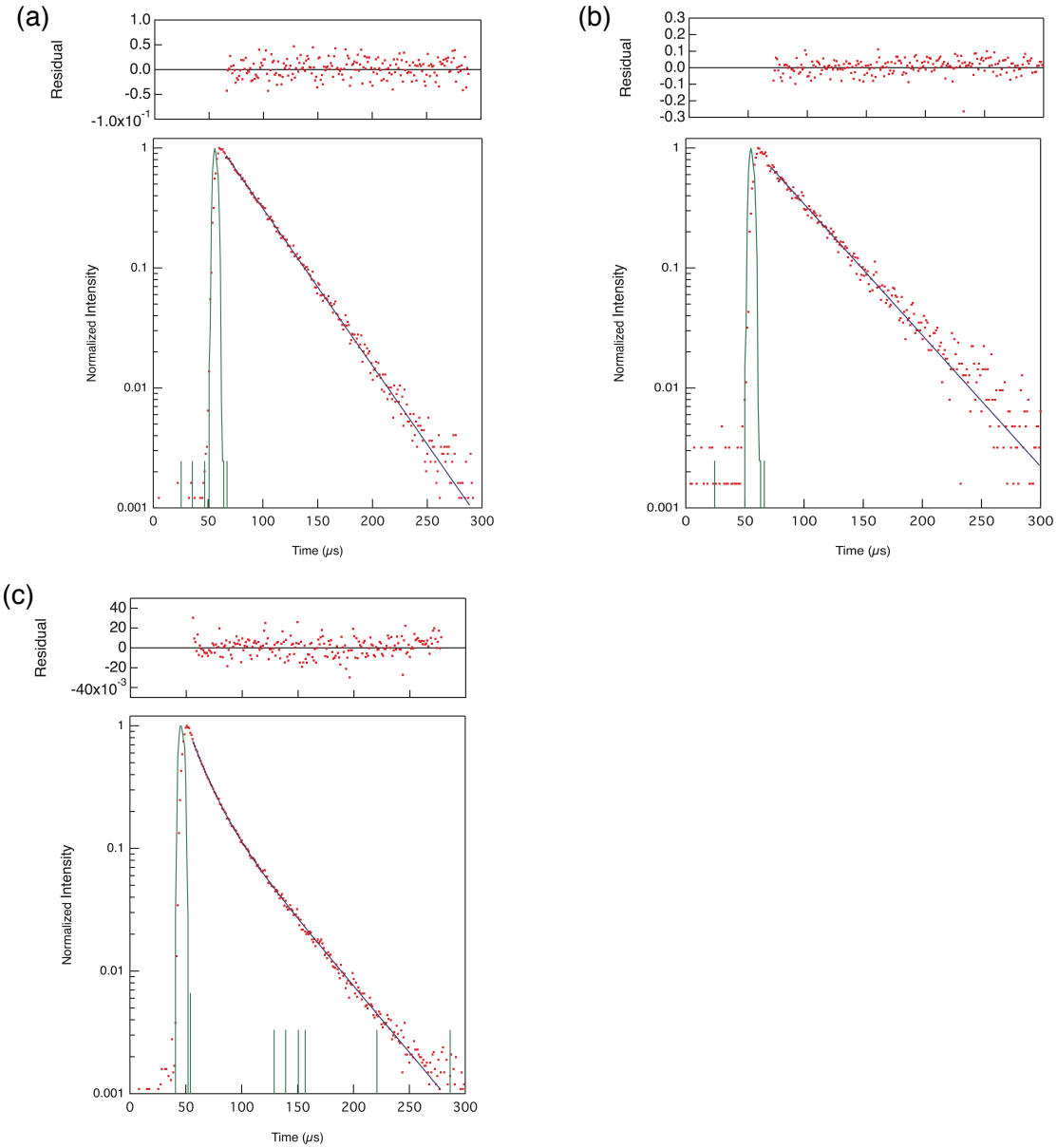

Fig. S10. Photoluminescence decay profiles of complexes **1a** (a), **1b** (b), and **1c** (c) at room temperature: excitation at 337 nm (pulse width 600 ps; 10 Hz).

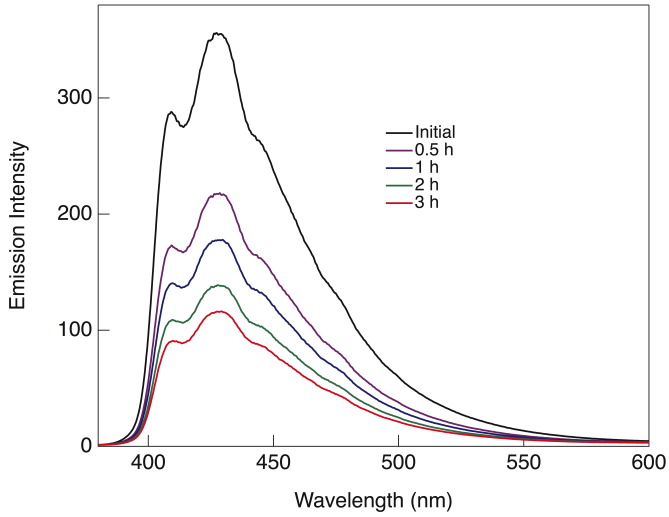

Fig. S11. Time course of photoluminescence spectra of complex **1c** in crystalline phase observed by continuous irradiation at 310 nm (6.5 mW cm^{-2}) at 20 °C in air.

References and Notes

(1) Coco, S.; Espinet, P.; Falagan, S.; Martinalvarez, J. M. *New J. Chem.* **1995**, *19*, 959.

(2) Howard, M. J.; Heirtzler, F. R.; Dias, S. I. G. *J. Org. Chem.* **2008**, *73*, 2548.